Projections for charm balance functions in heavy-ion collisions

Tilde Bonnevier Wallstedt

Thesis submitted for the degree of Bachelor of Science
15 hp

Supervisor: Alice Ohlson
Co-supervisor: Peter Christiansen

Department of Physics: Division of Particle Physics

May 2022

LUNDS
UNIVERSITET

Abstract

In this thesis, pp collisions were simulated using PYTHIA. D^+D^- and $D^0\overline{D^0}$ balance functions were created in order to contribute with a reference point for future balance functions measured in real data from Pb-Pb collisions. Charm balance functions are important since the charm quark can act as a probe of the QGP, probing the first instances after a collision. The balance functions were created under varying conditions: (i) minimum bias with only events with 2 charms, (ii) forcing charm production and (iii) forcing charm production with only events with 4 charms.

The results were mainly in line with expectations. The main deviation from expectations was that no away-side peak was found in minimum bias collisions, indicating that the distributions are dominated by NLO processes. This was not in line with real data from pp collisions from LHCb.

Popular science summary

The first milliseconds after the big bang the universe consisted of what is called the quark-gluon plasma (QGP for short). This is a state of matter just like solid, liquid and gas.

You may recall that the atomic nucleus consists of protons and neutrons. However, it does not stop there: these protons and neutrons in turn consist of particles called quarks. These are the smallest constituents of the universe, and they are bound together by something called gluons (as they act as the glue holding the quarks together). Hadrons is the general name of particles that consist of quarks: protons, neutrons, kaons, pions, etc. Quarks can be seen as the lego pieces forming the hadrons, and the gluons would then be the studs keeping the lego pieces together. At high enough temperatures the quarks and gluons stop being bound to hadrons, and they form this quark-gluon plasma. The QGP is like a hot, dense soup of quarks and gluons.

As mentioned previously, the QGP existed for the first milliseconds after the big bang. However, it can also be produced for a brief moment after collisions of heavy ions (such as Pb) due to the large amount of energy released during such a collision. ALICE (A Large Ion Collider Experiment) is an experiment at one of the world's largest particle accelerators: the LHC. At ALICE the products of heavy ion collisions are being detected partly for the reason of investigating the QGP. Investigating the particles and their distribution after such a collision can provide information about the plasma.

One specific type of quark is called the charm quark, and this type of quark is especially interesting when investigating the QGP. One of the reasons for this is that it is produced early in a collision, and can therefore provide information about the earliest stages of the collision: the stage when the QGP exists.

In this thesis particle collisions are being simulated and the resulting distribution of charmed hadrons are being investigated, to create what is called a balance function. A balance function tells us the following: if we have the position of a charmed hadron: where is its initial partner? Charm quarks are always created in pairs, so if we have detected a charmed hadron, we know that the charm quark in this hadron has an initial partner in some other hadron. This relationship between where in space a charm quark and its initial partner are located in the final state (the state the detector will be able to analyse) is what this balance function will tell us.

In this thesis it will be attempted to create as realistic simulations as possible, to imitate as closely as possible what it might look like in real data. Using data from LHC Run 3 (2022-2025) this type of balance function could be interesting to measure. To then compare the appearance of the balance function in the two settings: (i) LHC setting where we expect to see a QGP, and (ii) the setting from these simulations where we do not expect to see a QGP (since proton-proton collisions are being simulated), could provide information about how the QGP works. Aside from this, a prediction about how much data will be needed to create such a balance function from real data could be created.

To summarize: in this thesis the distribution of charmed hadrons after a heavy-ion collision is being investiated in hopes of being able to contribute with information about the QGP.

Contents

Chapter 1

Theory

1.1 Introduction

In this thesis balance functions (see Section 2.1) for charmed hadrons after pp collisions (proton-proton collisions) are studied, using PYTHIA (see Section 2.2.2) to simulate events. Investigations of this type are important for our understanding of pp collisions as well as heavy-ion (e.g. Pb-Pb) collisions, where we expect formation of a quark-gluon plasma (QGP). The purpose of this thesis is to contribute with knowledge of how much data will be required to create such balance functions from the real data from the LHC (Large Hadron Collider) [1], as well as contributing with material that one could compare the real Pb-Pb measurements with in the future, to observe how the presence of the QGP affects the distribution of particles.

1.2 Basic standard model theory

The standard model of particle physics describes the fundamental particles of the universe. The particles are divided into 4 groups: the gauge bosons, the scalar bosons, the leptons and the quarks [4].

1.2.1 The gauge bosons

The gauge bosons are the force carriers, meaning that elementary particles interact with one another though exchange of these bosons. The gauge bosons are: the massless photon (force carrier for the electromagnetic force), the massive W and the Z bosons (force carriers for the weak nuclear force), and the massless gluon (force carrier for the strong nuclear force). Gluons interact with particles with color charge, such as quarks. As they also carry color charge themselves this leads to gluon self-interactions. The gauge bosons all have spin 1. [4]

1.2.2 The scalar bosons

The scalar bosons is a group of elementary particles consisting of only one particle: the Higgs boson. The Higgs boson has 0 spin and is massive. It is produced by the Higgs field, and

interactions with the Higgs field is what gives some particles mass. Massless particles such as the photon do not interact with the Higgs field [4].

1.2.3 The leptons

The leptons are elementary particles with half-integer spin. They only interact via the electromagnetic and weak interactions. The leptons are: the electron e^-, the muon μ^-, the tau τ^-, and their respective neutrinos: the electron neutrino ν_e, the muon neutrino ν_μ, and the tau neutrino ν_τ. e^-, μ^- and τ^- all have electric charge -1 and interact weakly as well as electromagnetically. The neutrinos are all electrically neutral and interact weakly exclusively [4].

1.2.4 The quarks

Quarks are what makes up hadrons (protons, neutrons, etc). There are six types of quarks: up and down (1st generation), strange and charm (2nd generation), and top and bottom (3rd generation). Up, charm and top have electric charge $+2/3$, whereas down, strange and bottom have an electric charge of $-1/3$. They all have a spin of $1/2$. The quarks can interact via the strong interaction (exchange of gluons), as well as weakly and electromagnetically. Quarks carry a color charge: red, blue, green, anti-red, anti-blue or anti-green. Quarks possess a color and anti-quarks possess anti-color. The total color of a hadron (a particle consisting of quarks) has to add up to white. Hadrons with two valence quarks are called mesons, and hadrons with three valence quarks are called baryons [4].

1.3 Quantum Chromo-Dynamics

Quantum Chromo-Dynamics, QCD for short, is the study of the strong interaction between particles, i.e. the interactions between quarks and gluons. QCD is analogous to QED (Quantum Electro-Dynamics), the study of the electromagnetic force between particles. The strong force is carried by the gluon and interacts with particles with color charge, whereas the electromagnetic force is carried by the photon and interacts with particles with electric charge [4].

There are, however, certain vital differences between the workings of QCD and QED. The magnitude of the electromagnetic force (as well as the weak nuclear force and the gravitational force) decreases with the distance between the interacting particles, whereas the strong force does not. This is a defining property of QCD, and leads to color confinement. In fact, it is impossible to completely separate quarks. If two quarks, constituents of a hadron, attempt to escape one another this leads to the creation of jets, which are explained in section 1.4.2. Another difference is the fact that photons themselves do not carry electric charge, whereas gluons do carry color charge, resulting in gluon self-interaction. Asymptotic freedom is another property of QCD, separating it from QED. This is the reduction of the magnitude of the force as the length scale decreases [4].

1.4 Heavy-ion physics

Heavy-ion physics is the study of colliding heavy nuclei. At the LHC, ultrarelativistic heavy ions are being collided and the resulting particles after the collision may be studied. The nuclei become Lorentz contracted as they travel at relativistic speeds before the collision, and may be described as discs. The colliding nuclei consist of the gluons and quarks making up the nucleons inside the nuclei. However, they contain other particles as well, such as sea quarks. As such, the colliding nuclei are highly complicated objects [2].

The energy density resulting from the collision is very large and leads to a deconfinement of quarks and gluons, and an inability to describe them as constituents of any hadrons. Despite this, they are not completely free from one another, but one still denotes this as a deconfined state. This state of nearly free quarks and gluons after a highly energetic heavy-ion collision behaves as a hydrodynamic liquid with an extremely low viscosity, and has received the name "quark-gluon plasma", QGP for short. This QGP is what is thought to have made up the universe the first milliseconds after the big bang [2].

The development of the physics after a heavy-ion collision can be described in the following way: immediately after the collision there is a pre-equilibrium phase, after which a very hot QGP phase is entered. Once the system has cooled enough there will be what is called chemical freeze-out. Chemical freeze-out refers to a ceasing of inelastic interactions. After the chemical freeze-out point hadronization will occur: the recombination of quarks and gluons into hadrons. The system will continue to cool until the kinetic freeze-out point is reached: the point after which elastic interactions stop [5].

1.4.1 Quark-gluon plasma

The QGP medium exhibits a collective flow (see [13]), and heavy quarks propagating the medium interact with it by elastic and inelastic scattering. Low-momentum heavy quarks are expected to, to some extent, exhibit the collective flow behavior that the QGP has [7].

Due to asymmetric properties of a collision (i.e. non-central collision or fluctuations of the nuclei), after the collision there will be anisotropies in the pressure gradients, leading to a particle flow dominantly in azimuthal momentum distribution (see figure 1.1) [2].

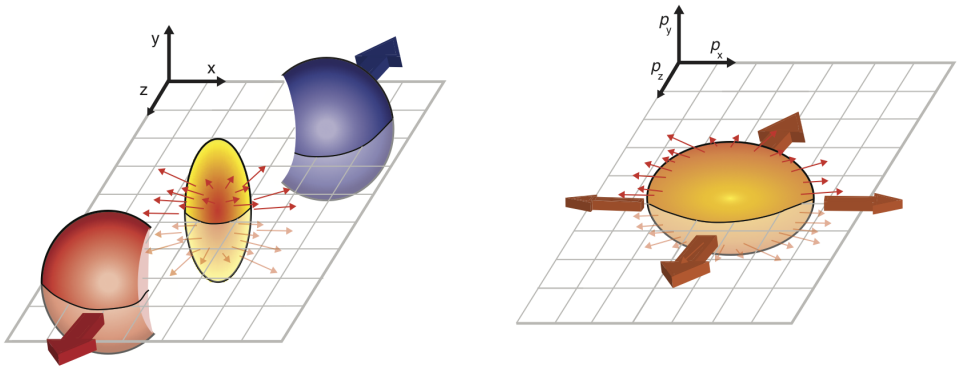

(a) Illustration with spatial coordinates (b) Illustration with momentum coordinates

Figure 1.1: Illustration of the anisotropic flow resulting from a non-central heavy-ion collision. Figure credit: B. Hippolyte

The anisotropy can be described using the following equation:

$$\frac{dN}{d\phi} = \frac{N}{2\pi}\left(1 + 2\sum_{n=1}^{\infty} v_n cos(n(\phi - \Psi_n))\right) \tag{1.1}$$

where Ψ_n is the n'th order symmetry plane, which is the angle perpendicular to the shape of the interaction region after the collision. ϕ is the azimuthal angle of the particles, v_n is the n'th anisotropic flow coefficient, and N is the average number of particles per event [2].

1.4.2 Jets

During a heavy-ion collision, hard scatterings lead to the production of jets. A jet is created when there is such an excess of energy that quark constituents of a hadron may attempt to escape one another. Due to color confinement, the strong force does not become weaker as the quarks attempt to escape the hadron. Thus, more and more energy is required to keep separating the quarks. Eventually, enough energy is present to create a quark/anti-quark pair out of the vacuum. These quark-pairs may continue the process, separating until there is enough energy to create another quark/anti-quark pair. Eventually, when there is not enough energy to keep the process going, there will be hadronization. This leads to jets ending up looking like clusters of high-momentum hadrons [2].

Jets are created during a heavy-ion collision due to the large amount of available energy, and these jets will interact with the QGP medium. The jets traversing the medium will lead to a suppression in the jet energy. This is called jet quenching, and has been observed experimentally [2].

1.5 Probing the QGP

1.5.1 The charm quark

Since the QGP exists for a very short time when created, in order to investigate it it is required to probe short timescales. From the Heisenberg uncertainty principle it follows that if one wants to examine short timescales, large energies are required. This can be obtained in two ways: high p_T (transverse momentum) light quarks (such as up, down or strange), or heavy quarks (such as charm or bottom). In this thesis the charm quark is used as a probe of the QGP. There are several advantages in using the charm quark for this purpose. Below some of these reasons are listed.

Charm quark/anti-quark pairs are created in the early stages of a heavy ion collision. A study of how charm quarks are distributed thus allows us to study the QGP phase of the collision [3].

Open charm (hadrons containing one charm quark) and charmonium (hadrons containing a charm and an anti-charm) production have large cross sections, which allows for good statistics [3].

Furthermore, the charm quark is known to interact with the medium, and the initial production of charm quarks can be estimated with high accuracy. The mentioned reasons make the charm quark a reasonable probe of the QGP [3].

1.5.2 The D meson

The D mesons have the quark content: $D^0 : c\overline{u}$, $\overline{D^0} : \overline{c}u$, $D^+ : c\overline{d}$, $D^- : \overline{c}d$, and it is the lightest charmed hadron. In order to use the charm quark as a probe of the QGP it is necessary to use a charmed hadron instead. This is because in an experiment (such as ALICE), the detector will reconstruct particles using their decay products. One will never experimentally observe a charm quark, but will observe for instance the decay products of a D^+ and be able to conclude that there was a D^+ meson at some point, and thus a charm quark.

In this thesis D mesons were used as probes, since they are the lightest charmed hadrons and will therefore be produced more often than other heavier charmed hadrons. One generally does not want to use baryons as probes, since the baryon number needs to be conserved and this adds another layer of difficulty, as the background will not be completely reduced by creating the balance function, which is explained in section 2.1.

1.6 The ALICE Experiment

ALICE [6] (A Large Ion Collider Experiment) is one of the experiments at LHC (Large Hadron Collider) at CERN. The main motivation for building ALICE was to investigate the QGP by detecting the products of highly energetic Pb-Pb collisions at LHC. Aside from this, ALICE also investigates collisions of lighter nuclei, as well as collisions of protons with nuclei. ALICE has 18 different detector systems. The systems are designed to cope with the

very high multiplicity of particles in Pb-Pb collisions [6].

There are two relevant observables in this study: the azimuthal angle (ϕ) and the pseudorapidity (η). The pseudorapidity is defined as $\eta = -ln\left(tan\left(\frac{\theta}{2}\right)\right)$ (where θ is the polar angle). The angles θ and ϕ are illustrated in figure 1.2. ϕ has the range (0,2π). The ALICE detector is cylindrical, and detects particles in pseudorapidity range η $(-0.8, 0.8)$. This region is called the acceptance region. η has the range (-0.8,0.8) in this thesis as well, to imitate the ALICE experiment [6].

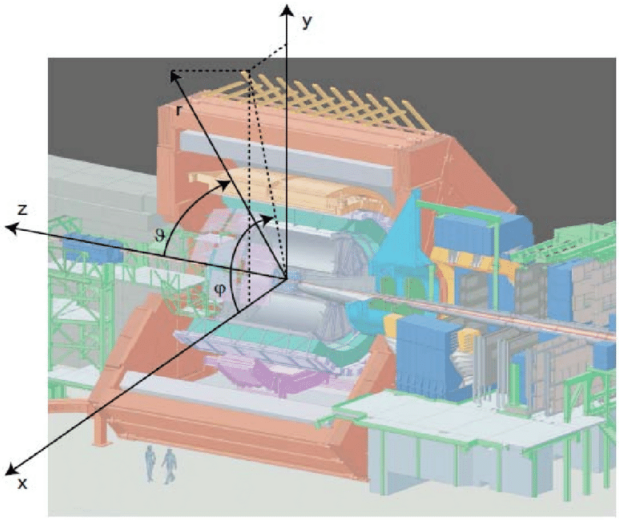

Figure 1.2: The ALICE detector layout. Image taken from [10]

The ALICE detector consists of a central barrel part and a forward muon spectrometer. The barrel part measures hadrons, electrons and photons. It is surrounded by a solenoid magnet. ALICE has an excellent tracking system, which consists of an inner tracking system (ITS) and a time projection chamber (TPC). These are the most important ALICE devices for detecting heavy-flavor particles [6].

1.6.1 Detecting D mesons in ALICE

In ALICE, one can reconstruct D mesons through the hadronic decay channels $D^0 \to K^-\pi^+$, $D^+ \to K^-\pi^+\pi^+$ and $D^{*+} \to D^0\pi^+$. [7]

The acceptance, Acc, of a detector is the percentage of the particles that fall inside the acceptance region. As mentioned, ALICE only detects particles in η between -0.8 and 0.8. The particles that fall outside this region will thus not be detected. The efficiency, ϵ of a detector is the percentage of the particles that do fall in the acceptance region that get detected. Thus, $Acc \cdot \epsilon$ gives the total percentage of particles that get detected, the *total efficiency*. A paper published in 2021 reported values of $Acc \cdot \epsilon$ for D^0 and D^+ mesons in ALICE for collisions with centralities of 0-10%. The reported values ranged between 10^{-3} at low p_T to 0.1-0.3 at higher p_T [7].

1.7 Correlation functions

Studying angular correlations between particles which initially came from the same hard scattering after a heavy-ion collision is a way of studying the QGP. A tool to investigate such correlations is what is called a correlation function. In a correlation function the position of a particle is correlated with the position of another. A way to do this is to correlate particles in $\Delta\phi$ and $\Delta\eta$ in 2D, or simply in $\Delta\phi$ in 1D. The correlation function is then defined as $\frac{d^2N}{d\Delta\phi d\Delta\eta}$. A peak at 0 and π in $\Delta\phi$ in a correlation function is a signature of a jet, since the average angular distance between particles from a jet will be 0 (from particles in the same jet) and π (from particles in back-to-back jets). The peak at 0 from a jet is referred to as the near-side jet peak, and the peak at π is referred to as the away-side jet peak. The correlation function between particles that are completely independent of one another (particles that are not from the same scattering) is expected to be flat [3].

1.8 The goal of this thesis

The goal of this thesis is to, by simulating proton-proton collisions in PYTHIA (section 2.2.2), create correlation functions for charmed hadrons and to analyse their appearance.

In proton-proton collisions (such as the ones simulated in PYTHIA in this thesis), a QGP is not expected to be formed since the collision is not energetic enough. However, using Pb-Pb data from LHC Run 3 (2022-2025), balance functions could be created for Pb-Pb collisions, where one expects to see a QGP, with real data. One could then compare the charm balance functions in the QGP setting to the charm balance function where we do not expect to see a QGP in order to extract properties of the QGP. The comparison is reasonable despite one being of type proton-proton and the other being of type Pb-Pb, since the statistics are expected to be the same regardless. This is because Pb-Pb collisions are a superposition of pp collisions with QGP modifications, and thus the hard scatterings will be the same. Thus, comparing the correlations between charm quarks in these two settings may allow us to observe how the QGP medium evolves over time.

Furthermore, since the statistics are expected to be the same, one can use the number of events required to create a reasonable balance function in PYTHIA to estimate the statistics required to create real balance functions with the LHC data.

Similar measurements with PYTHIA have been made in a paper published in 2021 [3]. However, in that paper all charm quarks were summed over to make the correlation function. This cannot be done experimentally, as what one will be able to detect is which final-state hadrons are present after the collision. Thus, measuring the correlation functions for specific hadrons allows us to imitate what the real data measurements will look like. This is what is done in this thesis.

Chapter 2

Method

2.1 Balance functions

Correlation functions were measured for the following types of particles: D^+D^-, $D^0\overline{D^0}$, $D^0\pi$, $\overline{D^0}\pi$. One mainly wants to investigate correlations between a hadron with a charm and a hadron with an anti-charm, since these are the quarks that will have originated from the same hard scattering. The intention is to measure the correlation between charm and anti-charm quarks ($c\overline{c}$). If one simply sums over all charm quarks and anti charm quarks and measures the angular difference between them, then one will also account for particles that are not related whatsoever that originate from different hard scatterings.

This is illustrated below in figure 2.1. Here 2 hard scatterings producing a charm/anti-charm pair are illustrated. If more than one scattering producing such a pair is produced, then correlating charm with anti-charm will lead to correlating particles that were not created in the same process (in addition to correlating particles that were created in the same process, of course). In the figure, for example, particles 3 and 1 are correlated, and 2 and 4 are correlated. However, simply correlating charm with anti-charm would assume a correlation between 2 and 3 as well as 1 and 4.

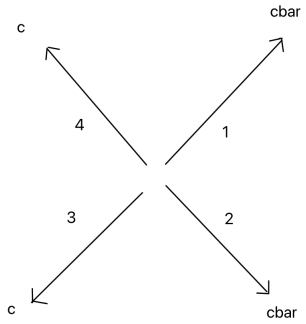

Figure 2.1: Loose illustration of two $c\bar{c}$ hard scatterings

In order to correct for this, one must do the following: correlate the opposite sign quarks with one another ($c\bar{c} + \bar{c}c$) and correlate the same sign quarks with one another ($cc + \overline{cc}$), and after this subtract them to get $[c\bar{c} + \bar{c}c] - [cc + \overline{cc}]$. The resulting correlation will be correlations between charms and anti-charms from the same hard scattering, and is called a *balance function*. This removes the background that arises from correlating uncorrelated particles. This is what was measured in this thesis. The balance functions measured were the ones mentioned previously: D^+D^-, $D^0\overline{D^0}$. Correlation functions were also made for $D^0\pi^+$, $\overline{D^0}\pi^+$, $D^0\pi^-$ and $\overline{D^0}\pi^-$. Below the measurements required to access the balance function for each of the correlations are listed:

Correlation	Measurement
D^+D^-	$[D^+D^- + D^-D^+] - [D^-D^- + D^+D^+]$
$D^0\overline{D^0}$	$[D^0\overline{D^0} + \overline{D^0}D^0] - [D^0D^0 + \overline{D^0}\overline{D^0}]$

2.2 Tools

2.2.1 ROOT

ROOT is a tool for data processing created at CERN, designed for particle physics data analysis. ROOT is used to store and process data. In this thesis ROOT is used with C++. [8]

2.2.2 PYTHIA

PYTHIA is a Monte Carlo Event Generator created at Lund University. Monte Carlo event generators make use of the random nature of physics, randomizing certain properties of the particles that are produced, of course within range of the possible properties and using probabilities to make the randomized values as realistic as possible. PYTHIA simulates

high-energy collisions in particle physics. The first stage of the development of PYTHIA started in 1978 with the development of JETSET [14] in Lund. This was the first part of the Lund Monte Carlo collection. Several programs have been based on JETSET, amongst others PYTHIA. In 1997 the programs were merged and called PYTHIA [9].

Part of the available simulations include proton-proton collisions. This is the part of PYTHIA that was utilized in this thesis. In such simulations, PYTHIA simulates realistic products of a proton-proton collision, and properties of the different particles, such as angle, transverse momentum, and particle type can be accessed [9].

One can access a certain type of particle after the collision by using the so-called PDG (Particle Data Group [15]) code of the particle. Each subatomic particle has a code; for example the PDG code of the D^0 meson is 421. Thus, one can tell the program to only save out tracks with PDG code 421, if the only interesting particle is the D^0. In this thesis this was partly utilized to create balance functions between certain types of particles, but it was also used to only save out the interesting particles so that the sample with the particle properties saved out did not take up unnecessary space [9].

2.3 Toy model

Before using PYTHIA to simulate particles, a Toy Model was built in C++ with ROOT to acquire an understanding of the processes that would be created with PYTHIA in the later stage of the project. What was done for the toy model was essentially creating a while-loop which iterated over i (set to 10 000) events. An event plane was randomly generated. 2 jets were simulated by randomizing angles in the angular directions η and ϕ. 100 particles per jet were randomly generated from a Gaussian distribution around the jet axis. 1000 more particles were generated according to Equation 1.1, to imitate the flow of QGP bulk particles. Correlation functions were made, correlating values in ϕ and in η.

2.4 Main method

The main part of the method consisted of simulating real pp collisions with PYTHIA with a collision energy of 13 TeV, and from them creating correlation functions for charmed hadrons. A varying number of events were simulated, saving out only the relevant particles. A for-loop looping over all events was created, within which a for-loop looping over all tracks (particles) was created. In these loops correlations were made between particles from the same event and from different events. Due to the ALICE acceptance region, a restriction was put on the values of η to lie between -0.8 and 0.8. One can, via PYTHIA, access properties of tracks, such as particle type, momentum, angle, etc. Two different types of histograms were filled for each particle correlation: same-event particle correlations and mixed-event particle correlations.

2.4.1 Same event vs mixed event particle correlations

The same-event histograms were filled with the angular difference ($\Delta\eta$ and $\Delta\phi$) between tracks from the same event, whereas the mixed-event histograms were filled with angular differences between tracks from different events. The truly relevant one is of course the same-event correlations, as one does not expect a correlation between particles created in different events.

However, there is a phenomenon which makes the mixed-event correlations relevant, which is called acceptance effects. The ALICE detector exclusively detects particles within the range (-0.8,0.8) in η. This implies that a smaller angle between particles leads to a higher probability of both of them falling within the acceptance region. A larger angle leads to a higher probability that one or both of the particles will fall outside the acceptance region, and will thus not be detected. This is the only correlation there will be between particles from different events. Therefore the correlation function between particles from different events will have a triangular appearance in $\Delta\eta$ with peak at 0, whereas it will be flat in $\Delta\phi$.

This acceptance effect will be present in the same-event correlation functions, but is of no physically interesting meaning, and one therefore wishes to eliminate it. This can be done by dividing the same-event correlation functions by the mixed-event correlation functions, since the mixed-event correlation function will only consist of these acceptance effects. In this way one acquires the "signal", e.g. what is interesting to observe.

2.4.2 Method summary

In this thesis, histograms for both mixed-event and same-event correlations were filled for all of the interesting particle correlations. The same-event histograms were divided by the mixed-event histogram to correct for acceptance effects.

Each histogram was normalized to get rid of the dependence of the histogram appearance on the pure number of events. The same-event histograms were normalized according to what is called the per-trigger yield. What this means is that, if for instance one takes the example of D^+D^- correlations, one divides the histogram with the total number of "trigger particles", that is the number of D^+ mesons. In this way one accesses the number of D^+D^- correlations per D^+ particle, rather than the total number of D^+D^- correlations. The mixed-event histograms were normalized such that the value at $(\Delta\phi, \Delta\eta) = (0,0)$ is 1.

For each correlation function, a one dimensional histogram in $\Delta\phi$ was filled as well. For the creation of these histograms, no mixed event division was performed.

Three different PYTHIA simulations were made (three different samples) with different conditions. In one sample the conditions were minimum bias, meaning that no charm quarks were forced and the program simulates realistic events such as the ones we might expect at LHC. In this sample, only events with 2 charm quarks (charm and anti-charm) were stored. This was done by requiring either at least one D^+D^- pair or at least one $D^0\overline{D^0}$ pair. Since the conditions were minimum bias, a lot of events with no charm quarks were produced,

which is why the condition was put that each event produced at least one $c\bar{c}$ pair. This sample was generated with 20 000 000 events.

In another sample, production of charm and anti-charm quarks was forced in each event by requiring the initial hard scattering in PYTHIA to be the process gg $\rightarrow c\bar{c}$ or qq $\rightarrow c\bar{c}$. This was done with the following lines of code (2.2):

```
pythia.readString("HardQCD:gg2ccbar = on");
pythia.readString("HardQCD:qqbar2ccbar = on");
```

Figure 2.2: Code for forcing charm production

This sample was generated with 10 000 000 events.

In a third sample, charm production was forced again, and in that sample only events with 4 charm quarks (two charm and two anti-charm) were saved out. This required generation of more events, in order to find enough events with multiple $c\bar{c}$ pairs produced. This sample was generated with 50 000 000 events.

Chapter 3

Results

3.1 Same events and mixed events

Below (figure 3.1) is an example of a same event and a mixed event histogram in 2D.

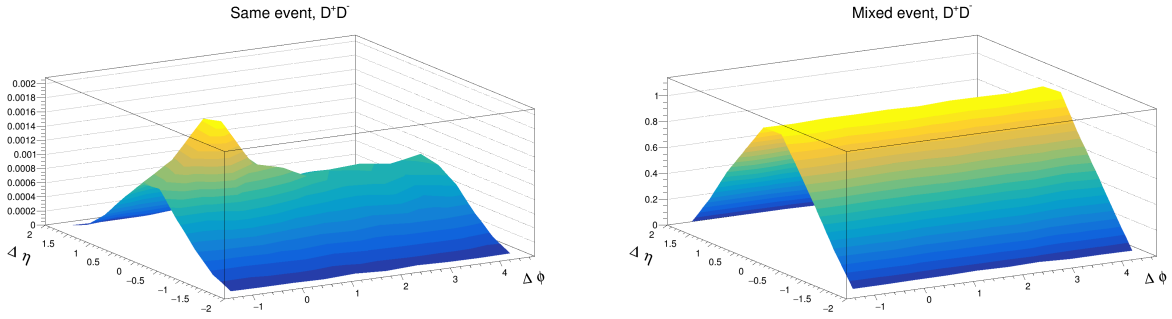

(a) Same-event correlation function, D^+D^- (b) Mixed-event correlation function, D^+D^-

Figure 3.1: Same-event and mixed-event 2D histograms, D^+D^-

The result of dividing the same-event histogram with the mixed-event histogram (when also subtracting the same-sign with the opposite-sign to obtain the balance function) is the following balance function (figure 3.2):

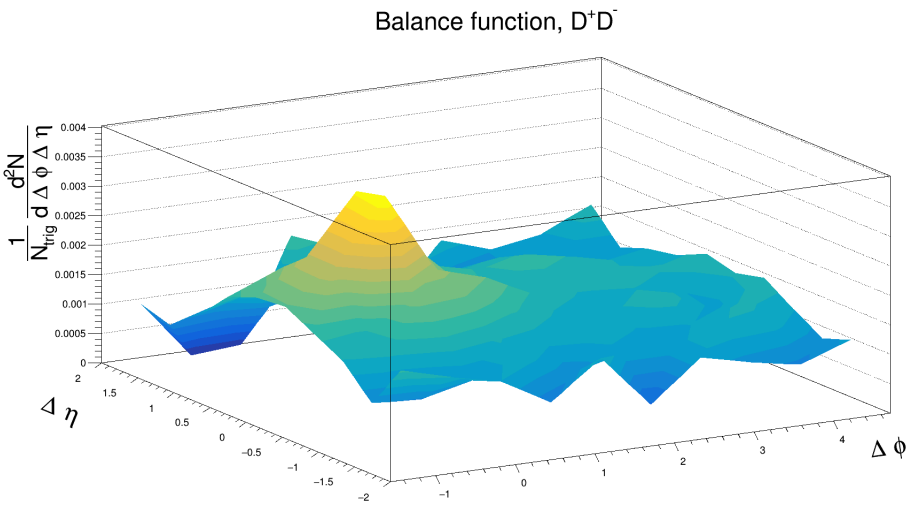

Figure 3.2: D^+D^- balance function, 2D

As can be seen, the mixed event histogram is triangular in $\Delta\eta$ and flat in $\Delta\phi$, as expected. The same event histogram is triangular in $\Delta\eta$ and has a peak at 0 in $\Delta\phi$. Dividing them results in removing the triangular behavior of the same-event histogram. In this thesis, the 1D histograms are mostly discussed, since these give clearer peaks. The rest of the 2D balance functions are displayed in Appendix A.

3.2 Minimum bias, storing events with 2 charm quarks

3.2.1 D^+D^- correlations

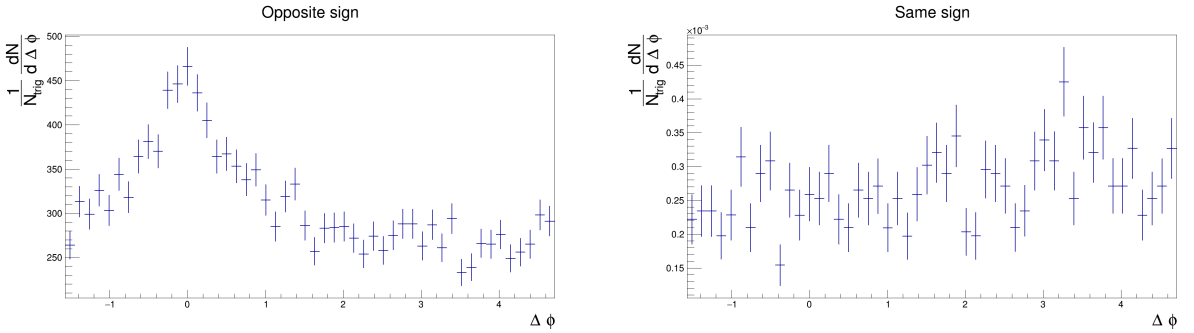

(a) $D^+D^- + D^-D^+$ correlation function

(b) $D^-D^- + D^+D^+$ correlation function

Figure 3.3: Same sign and opposite sign correlation functions, D^+D^-, sample 1

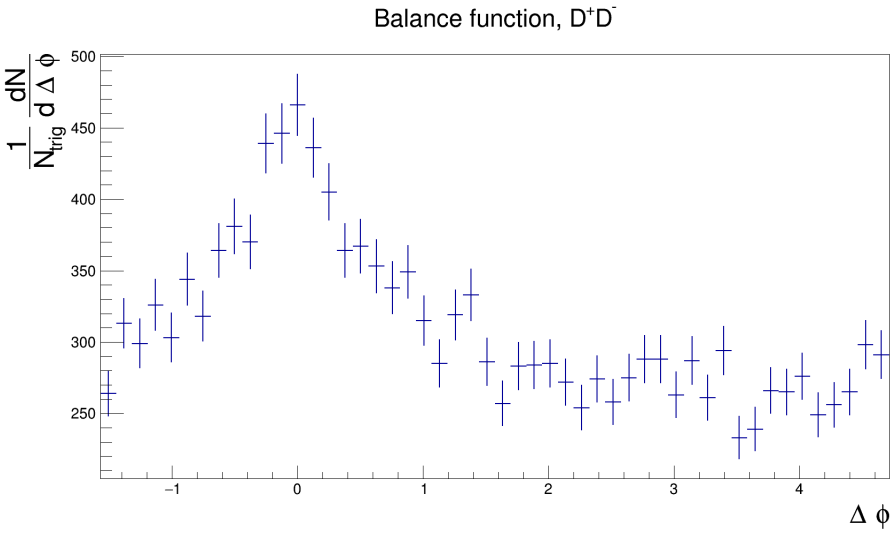

Figure 3.4: D^+D^- balance function in 1D, sample 1

The balance function shown in figure 3.4 has a clear near-side peak and no away-side. This sample was in minimum bias, meaning that charm/anti-charm pairs were created through natural processes. When the gluons or quarks that create a $c\bar{c}$ pair have large momentum, due to conservation of momentum, the charm and anti-charm would be created with only a small angle between them, creating a near-side peak and no away-side. This type of interaction is called **next-to-leading order (NLO)**. It is called next-to-leading order since these processes are not produced in the initial hard scattering, but from fragmentation of high-p_T particles after the initial collision. The peak in the balance function above is probably the result of such NLO interactions.

3.2.2 $D^0\overline{D^0}$ correlations

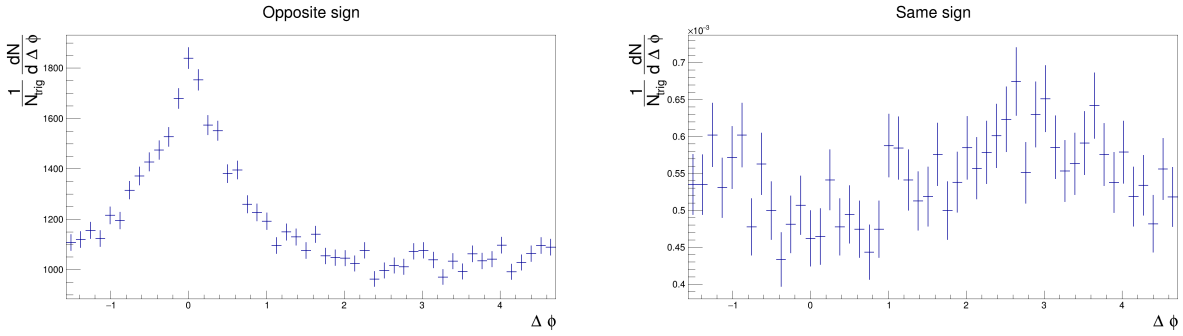

(a) $D^0\overline{D^0} + \overline{D^0}D^0$ correlation function

(b) $D^0D^0 + \overline{D^0D^0}$ correlation function

Figure 3.5: Same sign and opposite sign correlation functions, $D^0\overline{D^0}$, sample 1

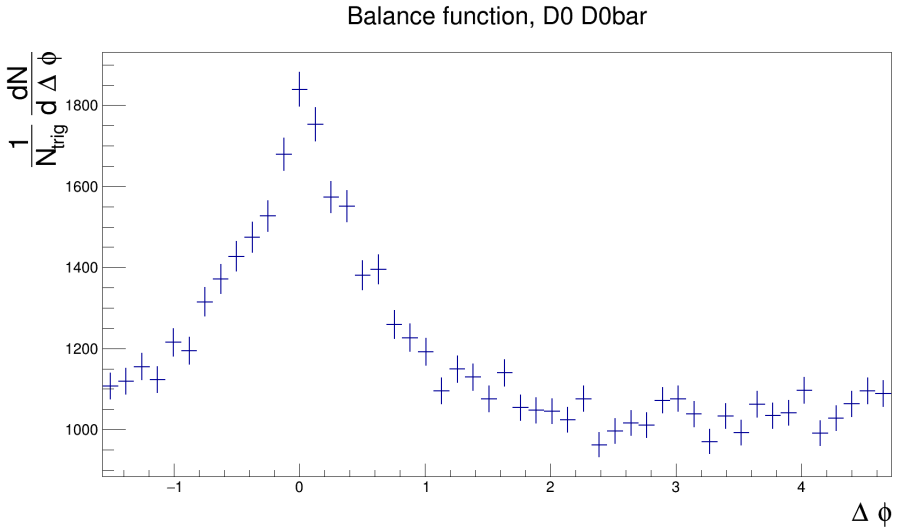

Figure 3.6: $D^0\overline{D^0}$ balance function in 1D, sample 1

The results for the $D^0\overline{D^0}$ in figures 3.5 and 3.6 are, as expected, similar to the results for D^+D^-. We expect them to be similar since both of the correlations correlate a meson with one charm with a meson with one anti-charm. The only difference between the two correlations is the difference between a $u\overline{u}$ pair from the $D^0\overline{D^0}$ correlation and a $d\overline{d}$ pair from the D^+D^- correlation. The up and down quark are both first generation quarks and are expected to behave similarly.

3.3 Forcing charm production

3.3.1 D^+D^- correlations

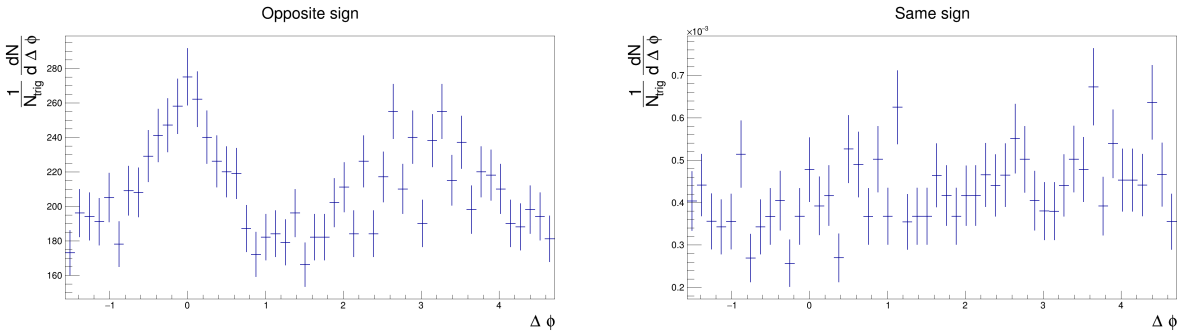

(a) $D^+D^- + D^-D^+$ correlation function

(b) $D^-D^- + D^+D^+$ correlation function

Figure 3.7: Same sign and opposite sign correlation functions, D^+D^-, sample 2

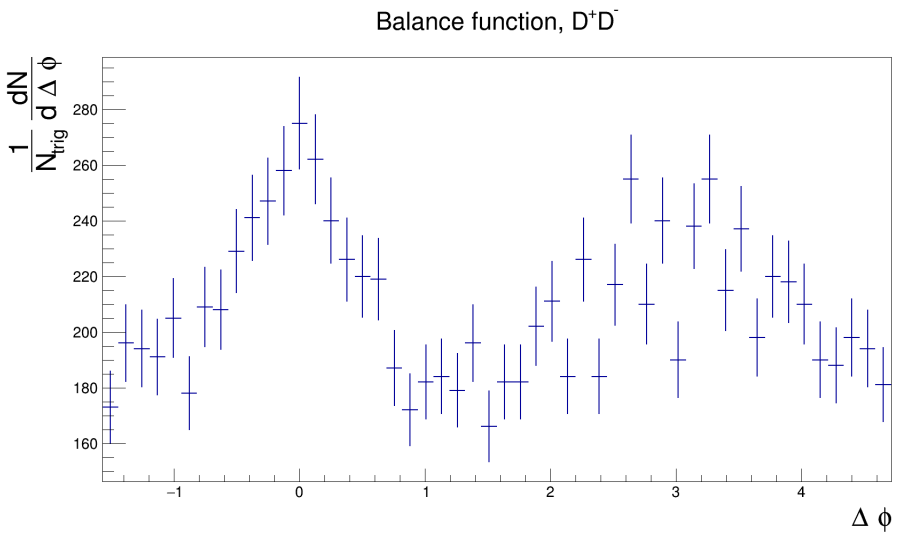

Figure 3.8: D^+D^- balance function in 1D, sample 2

The balance function from forcing charm production and saving out all events (figure 3.8) has a clear near-side and away-side peak, the near-side dominating. When PYTHIA forces charm production, it is forced in the initial hard scattering which means they will be produced close to the center-of-mass frame. Due to conservation of momentum, they will therefore be back-to-back. This type of interaction is called **leading order (LO)**. This is most likely where the away-side peak in this histogram arises from. Even though charm production is forced in this sample, NLO charm production from quark or gluon fragmentation will still occur as these cannot be removed, and this is most likely where the near-side peak originates from.

3.3.2 $D^0\overline{D^0}$ correlations

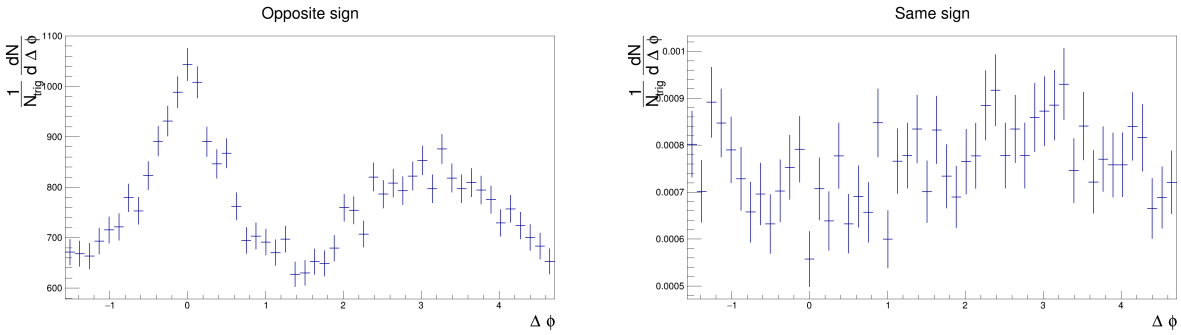

(a) $D^0\overline{D^0} + \overline{D^0}D^0$ correlation function

(b) $\overline{D^0D^0} + D^0D^0$ correlation function

Figure 3.9: Same sign and opposite sign correlation functions, $D^0\overline{D^0}$, sample 2

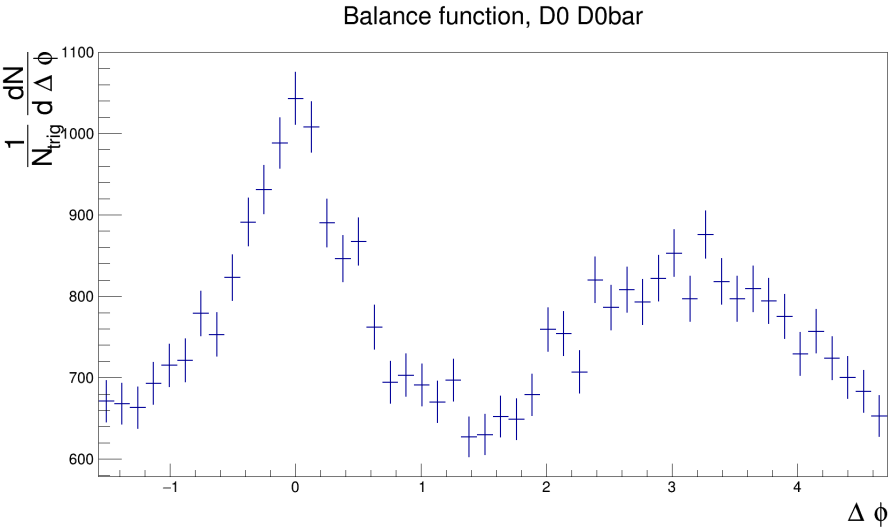

Figure 3.10: $D^0\overline{D^0}$ balance function in 1D, sample 2

The behavior of the $D^0\overline{D^0}$ correlations is very similar to that of the D^+D^- correlations, as expected. The reason that we expect such a similarity is explained in section 3.1.2.

3.3.3 $D-\pi$ correlations

$D-\pi$ correlation functions give us a comparison between (i) correlation functions between a charmed meson and another charmed meson ($D-D$), and (ii) correlation functions between a charmed meson and a non-charmed meson ($D-\pi$). The difference in the plots is thus the product of the loss of a charm quark. The reason that there is a correlation between D mesons and pions is production of jets.

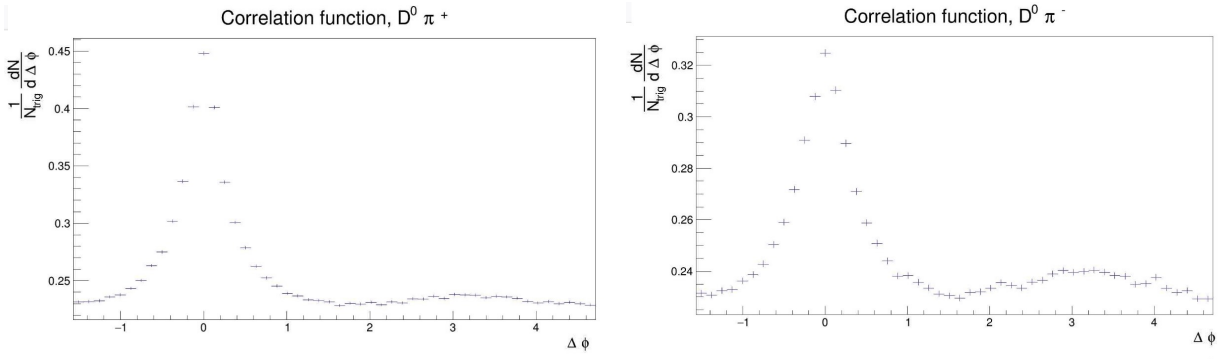

(a) $D^0\pi^+$ correlation function

(b) $D^0\pi^-$ correlation function

Figure 3.11: Correlation functions for $D^0\pi^+$ and $D^0\pi^-$

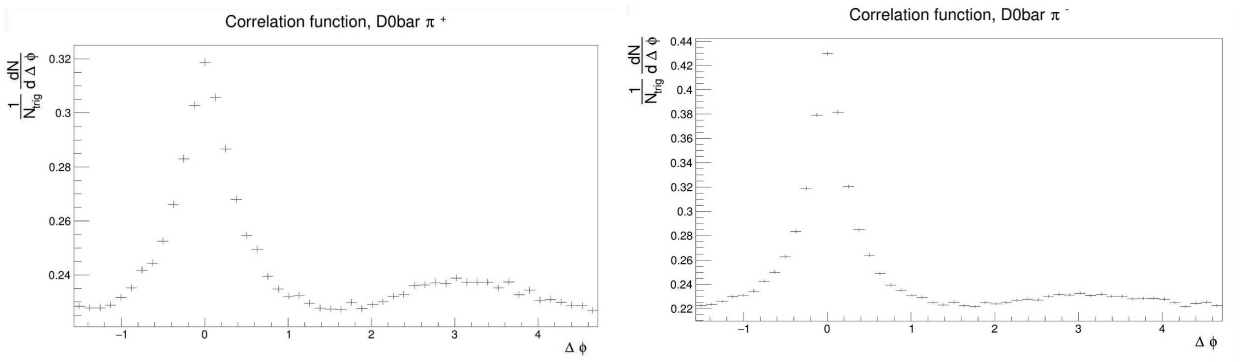

(a) $\overline{D^0}\pi^+$ correlation function

(b) $\overline{D^0}\pi^-$ correlation function

Figure 3.12: Correlation functions for $\overline{D^0}\pi^+$ and $\overline{D^0}\pi^-$

Above (figures 3.11 and 3.12) are correlations for D mesons with pions. The quark content of D^0 is $c\overline{u}$ and the quark content of $\overline{D^0}$ is $\overline{c}u$. The quark content of π^+ is $u\overline{d}$ and the quark content of π^- is $\overline{u}d$. Therefore correlating D^0 with π^+ should give a similar appearance as correlating $\overline{D^0}$ with π^-, since these correlations both correlate up with anti-up. Similarly, correlating $\overline{D^0}$ with π^+ should have a similar appearance as correlating D^0 with π^-, since these correlate up with up and anti-up with anti-up.

One would expect a more significant correlation for $D^0\pi^+$ (3.11a) and $\overline{D^0}\pi^-$ (3.12b) than for $D^0\pi^-$ (3.11b)and $\overline{D^0}\pi^+$ (3.12a) for the mentioned reason of the first 2 having a $u\overline{u}$ pair and the other two not having this. This is what we can observe in the histograms, as the value of the correlation function reaches 0.45 for the first two mentioned whereas it reaches 0.32 for the last two mentioned.

3.4 Forcing charm production, storing events with 4 charm quarks

3.4.1 D^+D^- correlations

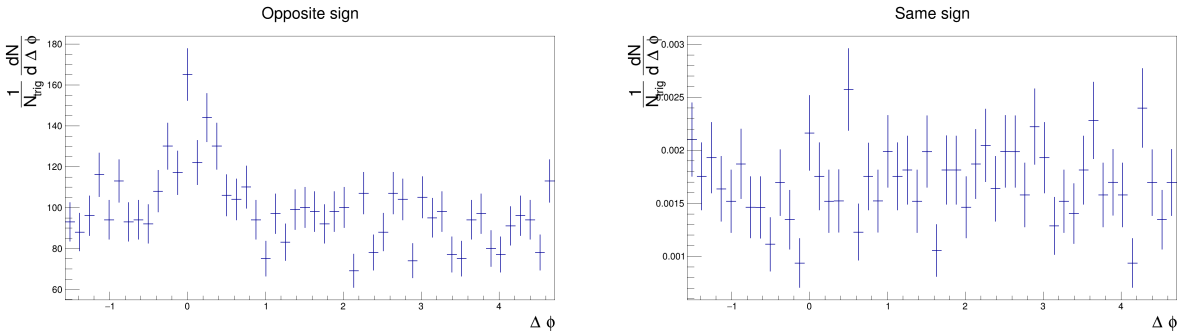

(a) $D^+D^- + D^-D^+$ correlation function

(b) $D^+D^+ + D^-D^-$ correlation function

Figure 3.13: Same sign and opposite sign correlation functions, D^+D^-, sample 3

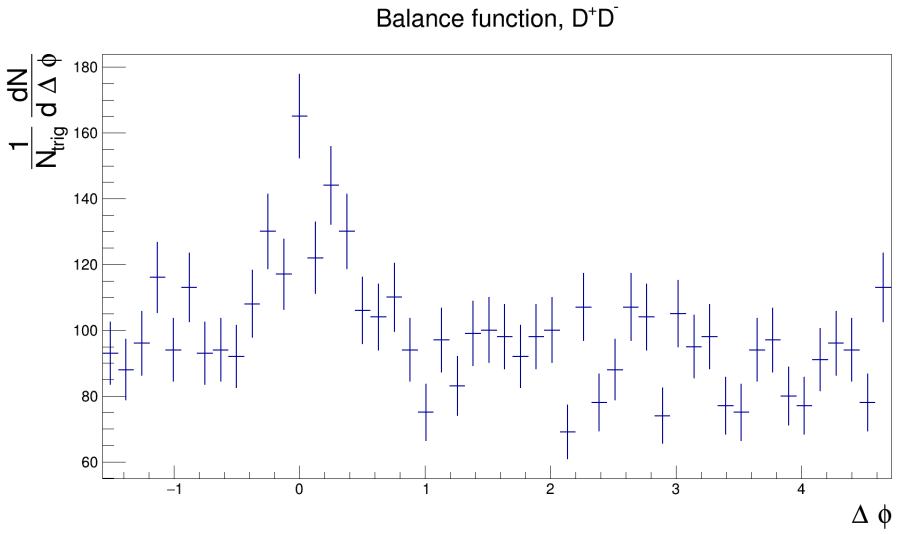

Figure 3.14: D^+D^- balance function in 1D, sample 3

The away-side peak that appeared in the plot from the second sample where charm was forced (figure 3.8) became less clear in the balance function for the sample where charm was forced but only events with at least 2 pairs of $c\bar{c}$ was saved (3.14). However, due to a lack of statistics it is not possible to completely exclude there being an away-side peak. One would expect an away-side peak, as one expects the process of forcing charm quarks back-to-back to still be present under these conditions.

3.4.2 $D^0\overline{D^0}$ correlations

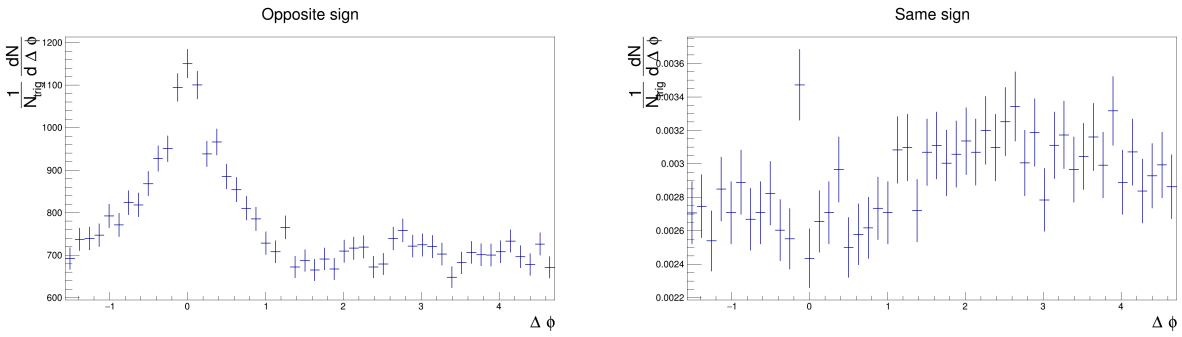

(a) $D^0\overline{D^0} + \overline{D^0}D^0$ correlation function

(b) $\overline{D^0D^0} + D^0D^0$ correlation function

Figure 3.15: Same sign and opposite sign correlation functions, $D^0\overline{D^0}$, sample 3

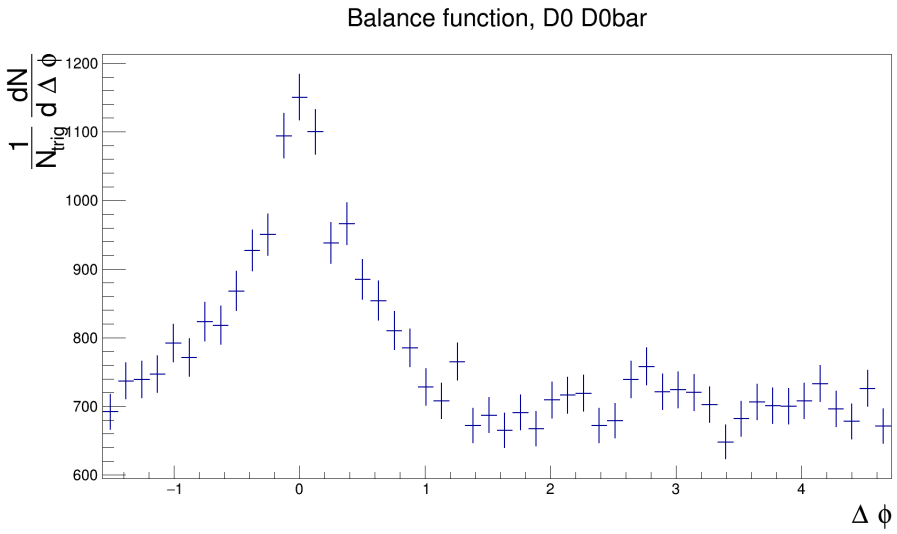

Figure 3.16: $D^0\overline{D^0}$ balance function in 1D, sample 3

Once again one can observe that the $D^0\overline{D^0}$ balance function (3.16) is very similar to the D^+D^- balance function (3.14).

3.5 Comparisons

As mentioned, we expect no significant difference between the D^+D^- correlation functions and the $D^0\overline{D^0}$ correlation functions, since these both correlate a charmed meson with an anti-charmed meson. This is also what is observed in the results. However, there are a lot more entries in the histograms for $D^0\overline{D^0}$ than in the histograms for D^+D^-. This implies that hard scatterings of $c\bar{c}$ are more likely to result in production of a $D^0\overline{D^0}$ pair than a D^+D^- pair.

The difference between events in minimum bias and events where charm quarks are forced from the program is clear from the results, one resulting in leading order behavior on top of next-to-leading order behavior, and the other resulting in only next-to-leading order behavior.

Chapter 4

Discussion

4.1 Projections for real data

As mentioned in Section 1.6.1, the ALICE detector has a total efficiency for detecting D mesons of around 10^{-3} for low-p_T to 0.1-0.3 for higher p_T. The most reasonable comparison to make with real data will be the simulations in minimum bias, since charm quark production cannot be forced in nature. The minimum bias sample was generated with 20 000 000 events. Thus, in order to achieve plots similar to the ones created in this thesis, one would need $\frac{20000000}{10^{-3}} = 2 \cdot 10^{10}$ to $\frac{20000000}{0.3} = 67 \cdot 10^6$ events.

However, since the real data would be taken from Pb-Pb collisions, not pp collisions, fewer events are actually required. To acquire the number of Pb-Pb events needed per pp event one must scale by the number of pp collisions in one Pb-Pb collision (N_{coll}). The value of N_{coll} varies depending on the centrality of the collision. For centralities of 0-5% it has a value of 1763, and for centralities of 20-30% it has a value of 592.7 [12].

Total efficiency	Centrality	N_{coll}	N_{events}
0.3	0-5%	1763	37800
0.3	20-30%	592.7	112000
10^{-3}	0-5%	1763	11300000
10^{-3}	20-30%	592.7	33700000

In the table above it is displayed how many events would be required for different centralities and efficiencies, to from Pb-Pb collisions create similar balance functions to the ones in this thesis. The lowest value lies at around 38 000 events and the highest at around $34 \cdot 10^6$ events. For reference, in a previous data analysis of Pb-Pb collisions from ALICE, data from $100 \cdot 10^6$ events was available [7].

4.2 Comparisons with previous results

4.2.1 LHCb

LHCb has previously measured correlation functions for D^+D^- and $D^0\overline{D^0}$ from pp collisions at 7 TeV. In this section these results are compared with the results from this thesis.

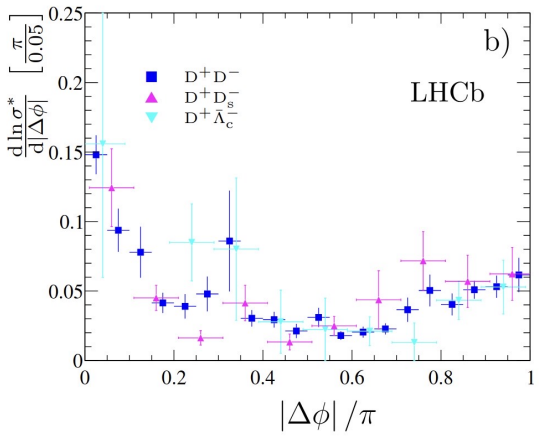

(a) D^+D^- correlation function from LHCb. Image taken from [11]

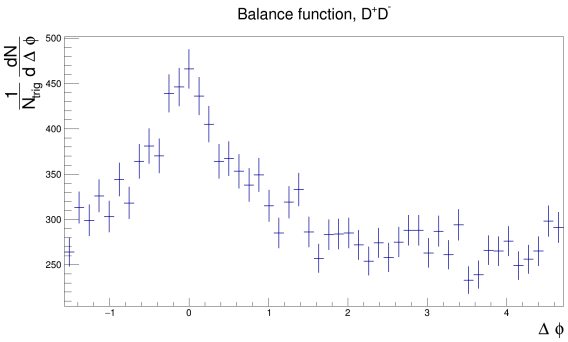

(b) D^+D^- balance function from this thesis

Figure 4.1: Comparison with LHCb, D^+D^- balance function

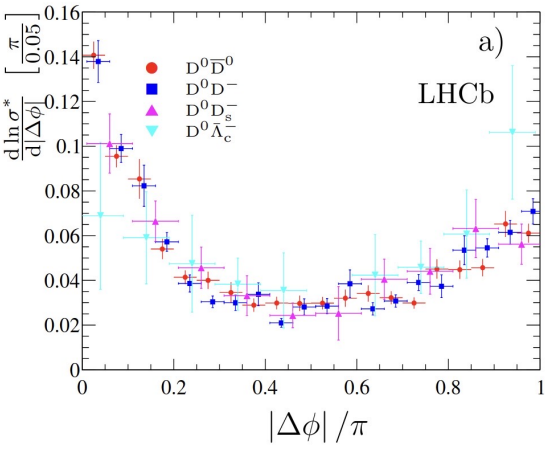

(a) $D^0\overline{D^0}$ correlation function from LHCb. Image taken from [11]

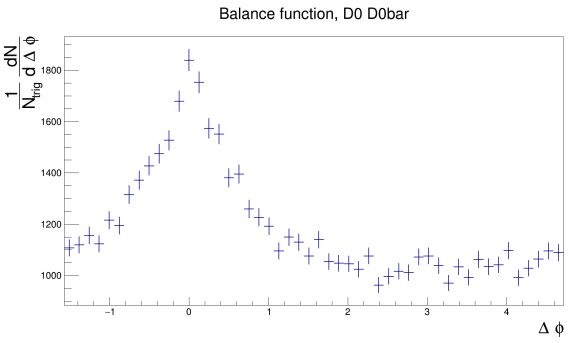

(b) $D^0\overline{D^0}$ balance function from this thesis

Figure 4.2: Comparison with LHCb, $D^0\overline{D^0}$ balance function

It can be observed from figures 4.1 and 4.2 that the data from LHCb gives a small but clear away-side peak that the PYTHIA simulations do not display. This indicates that there are some inconsistencies between PYTHIA and nature: perhaps not all of the cross sections for all types of events are correct in PYTHIA. PYTHIA seems to indicate that events of the type that lead to a small angle between particles are almost completely dominating in minimum bias. In the LHCb data the near-side peak is also greater than the away-side, however the away-side is clearly visible in a way that is not observed in PYTHIA.

4.2.2 Simulated charm balance functions

A paper was published in 2021, displaying charm balance functions measured in PYTHIA. [3] The method that they used was simply creating a balance function from all charm quarks, not of any specific mesons. The results differ a bit from the ones in this thesis. In said paper, charm production was forced. Thus, the most suitable comparison to make is to compare those plots with the ones where charm was forced in this thesis. In the paper, the results gave a clear away-side peak and no near-side peak. The results from this thesis gave a clear away-side, but a near-side that was even larger than the away-side. The reason behind this difference is that in the 2021 paper, only events with a maximum of 1 $c\bar{c}$ pair were stored. This in combination with forcing the initial hard scattering to produce a $c\bar{c}$ pair leads to this initial pair being the only pair in the event. This means that all $c\bar{c}$ pairs were created from LO processes, creating only an away-side peak and no near-side.

4.3 p_T dependence

A p_T spectrum was created (see figure 4.3). The two lines at the top represent D^0 and $\overline{D^0}$, whereas the two at the bottom represent D^+ and D^-.

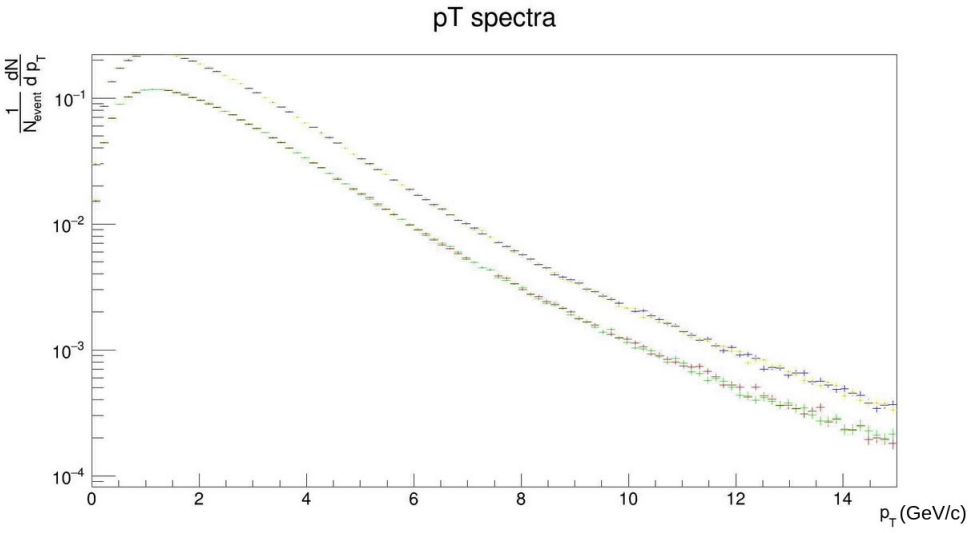

Figure 4.3: p_T spectrum

A p_T cut was implemented, such that the histograms only were filled for particles with $p_T > 2$ GeV. This will most likely be a more realistic depiction of the balance function that can be measured in real data. This is because it is more difficult to reconstruct and detect particles with very low p_T. The result of the p_T cut is shown below in figure 4.4, for the $D^0\overline{D^0}$ balance function in minimum bias.

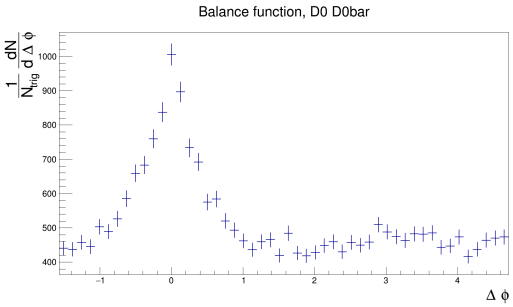

(a) $D^0\overline{D^0}$ balance function with p_T cut, 1D

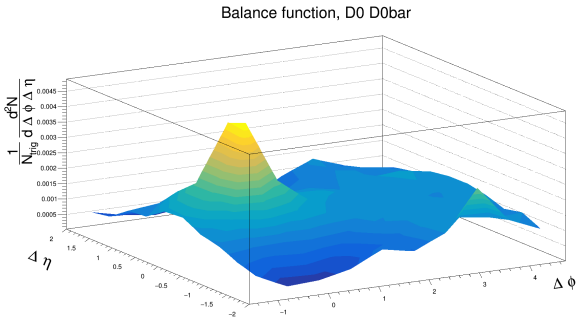

(b) $D^0\overline{D^0}$ balance function with p_T cut, 2D

Figure 4.4: $D^0\overline{D^0}$ balance function with p_T cut

Comparing the above figures with 3.6, one can see that the peak appears higher relative to the background with the p_T cut than without it, and a bit narrower. The rest of the balance functions with p_T cut are displayed in Appendix B.

4.4 Making the simulations more realistic

In the samples used in this thesis, not only final state particles were saved out. This means that a portion of the particles might actually have decayed into something else by the time the time the detector would detect them. In ALICE, of course only final state particles can be detected. This could contribute to a difference between real ALICE data and the simulations in this thesis.

Another source of uncertainty is PYTHIA inaccuracies. PYTHIA takes into account cross sections of different interactions and attempts to recreate as accurately as possible, using the Monte Carlo method, the processes after a pp collision. Of course, not everything that PYTHIA assumes will be 100% correct and mimic reality. For instance, as was discussed above, there are some inaccuracies that lead to differences between PYTHIA simulations and real data from LHCb.

Since all measurements were made using simulations, no standard measurement uncertainties are present. All uncertainties will be uncertainties in the way that PYTHIA has interpreted data and implemented into their model. However, all of the cross sections and all of the physics that PYTHIA have implemented are of course taken from real data, and in that sense PYTHIA will have adopted all of the uncertainties from these real measurements as well.

Chapter 5

Conclusion and outlook

Balance functions from pp collisions were created using PYTHIA, for D^+D^- as well as $D^0\overline{D^0}$ correlations. Additionally, correlations between D^0 and pions were made. In minimum bias, only near-side peaks were observed, indicating a dominance of NLO interactions. This was not in line with what was observed in LHCb in real data, indicating a difference between PYTHIA and nature. When charm production was forced, a smaller away-side appeared as a result of the LO interactions resulting from the way that PYTHIA forces the production.

The results of this thesis can act, keeping in mind the mentioned inconsistencies PYTHIA has with real data, as a reference point in the future if real charm balance function were to be created from ALICE data. The evolution of the charm balance function as one goes from pp collisions to Pb-Pb collisions could give us insight into the evolution of the QGP, since the charm quark is produced early in the collision and can act as a probe. Additionally, the results from this thesis also give us an idea of how the hard processes look in heavy-ion collisions, since these are expected to be similar to the ones in pp collisions.

The obvious next step is to attempt to recreate similar charm balance functions from ALICE data. Doing so and comparing the results with the results from this thesis allows us to use the charm quark as a probe of the QGP, which has a lot of advantages, as mentioned in Section 1.5.

Acknowledgements

Firstly, I would like to thank my supervisor Alice Ohlson for allowing me to do this project with her. She has been very patient and pedagogical, and has been available to meet up probably more often than others would be willing to. Thanks to her I have felt like this process has gone smoothly and has been very educational.

A big thank you to my co-supervisor Peter Christiansen as well, for being willing to discuss the results and give his expertise on the subject.

Lastly, I would like to thank my friend and fellow student Axel Helgstrand for always being down to discuss any questions I have on the subject, and for reading my thesis and giving his input.

Bibliography

[1] CERN. CERN *The Large Hadron Collider*. 2022. https://home.cern/science/accelerators/large-hadron-collider. (Retrieved 2022-05-20).

[2] Busza, W et al. Heavy Ion Collisions: The Big Picture and the Big Questions. *Annual Reviews*. 018. 68:1–49.

[3] Basu, S. et al. Probing the Gluon Plasma with Charm Balance Functions. *European Physical Journal C* . 2021

[4] B.R Martin and G. Shaw. *Particle Physics*. 4th edition. Chichester: John Wiley & Sons, 2017.

[5] Kumar, L. Systematics of kinetic freeze-out properties in high energy collisions from STAR. *Nuclear Physics A*. Vol. 931, 2014: p. 1114-1119. doi: https://doi.org/10.1016/j.nuclphysa.2014.08.085

[6] The ALICE Collaboration. The ALICE experiment at the CERN LHC. *IOP Publishing*. Vol. 3, nr. 08, 2008: p. S08002–S08002. doi: 10.1088/1748-0221/3/08/s08002

[7] The ALICE Collaboration. Prompt D0, D+, and D+ production in Pb–Pb collisions at $\sqrt{s_{NN}} = 5.02$ TeV. *JHEP*. Vol. 01, 2022. doi: 10.1007/JHEP01(2022)174

[8] CERN. ROOT. *About ROOT*. 2021. https://root.cern/about/. (Retrieved 2022-05-11).

[9] Sjöstrand, T. 2019. The PYTHIA Event Generator: Past, Present and Future. *Computer Physics Communications*. Vol. 246, 2020. doi: 10.1016/j.cpc.2019.106910

[10] Cavicchioli, C. Development and Commissioning of the Pixel Trigger System for the ALICE Experiment at the CERN Large Hadron Collider. 2010.

[11] The LHCb collaboration. Observation of double charm production involving open charm in pp collisions at $\sqrt{s} = 7$ TeV. *JHEP*. Vol. 06, 2012.

[12] The ALICE Collaboration. Centrality determination in heavy ion collisions. ALICE-PUBLIC-2018-011. 2018.

[13] Herrmann, Norbert et. al. Collective flow in heavy-ion collisions. *Annual Review of Nuclear and Particle Science*. Vol. 49, nr. 1, 1999: p. 581-632. doi: 10.1146/annurev.nucl.49.1.581

[14] Torbjörn Sjöstrand. PYTHIA 5.6 and JETSET 7.3: Physics and manual.

[15] Zyla, P.A. et. al. Particle Data Group. Review of Particle Physics. *PTEP*. Vol. 2020, nr. 8, 2020: p. 083C01.

Appendix A

2D plots

A.1 Minimum bias, storing events with 2 charm quarks

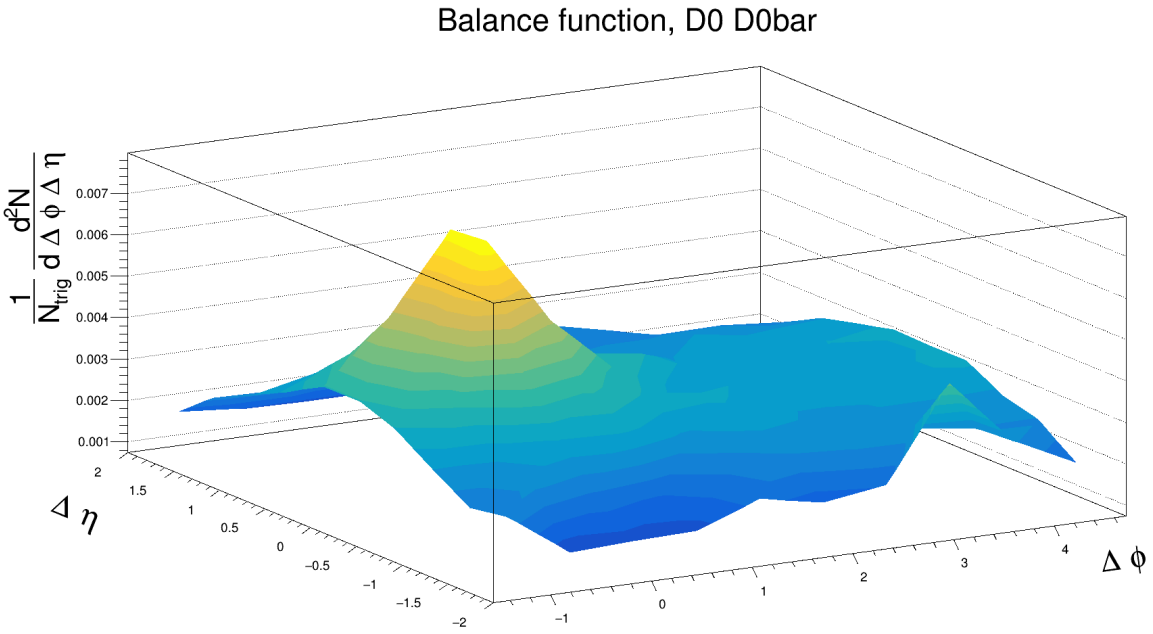

Figure A.1: $D^0\overline{D^0}$ balance function, 2D, sample 1

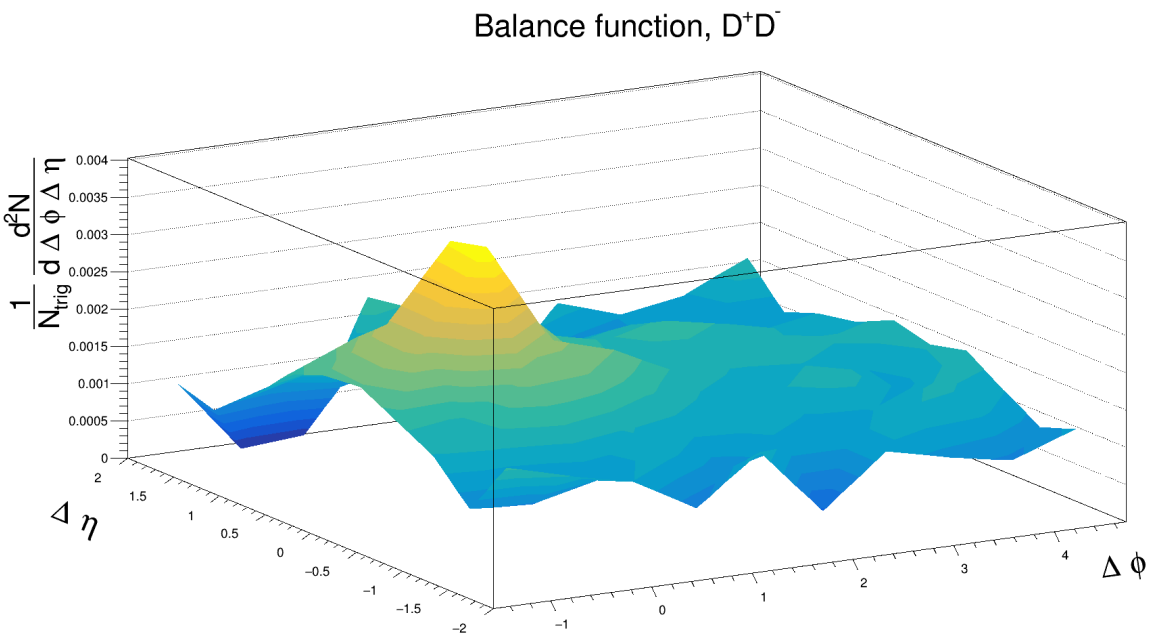

Figure A.2: D^+D^- balance function, 2D, sample 1

A.2 Forcing charm production

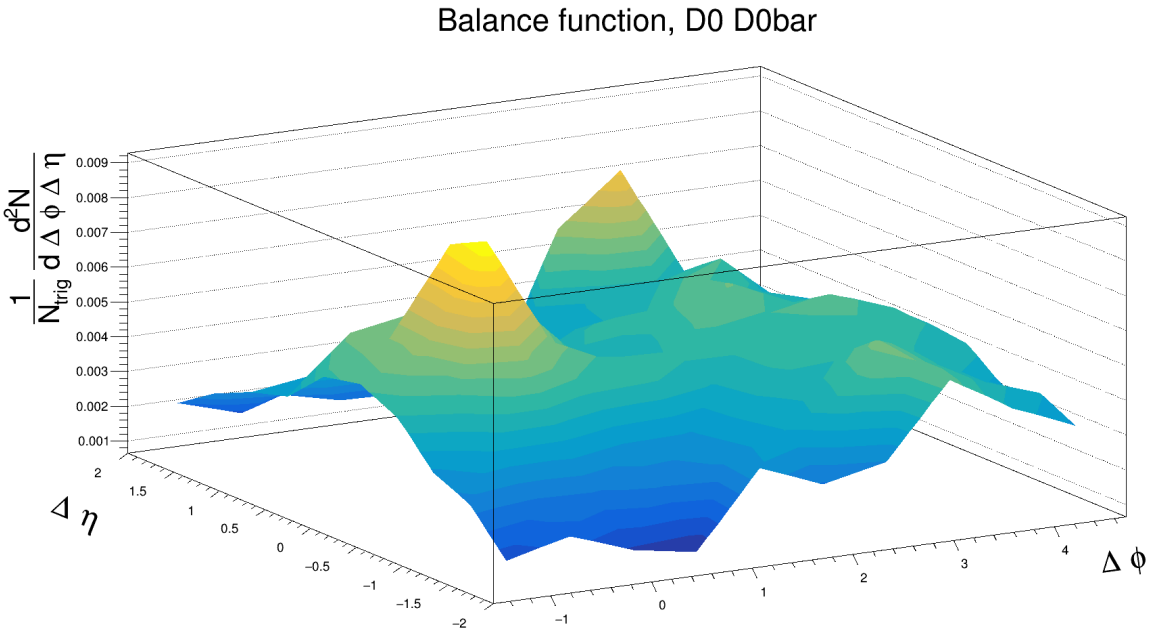

Figure A.3: $D^0\overline{D^0}$ balance function, 2D, sample 2

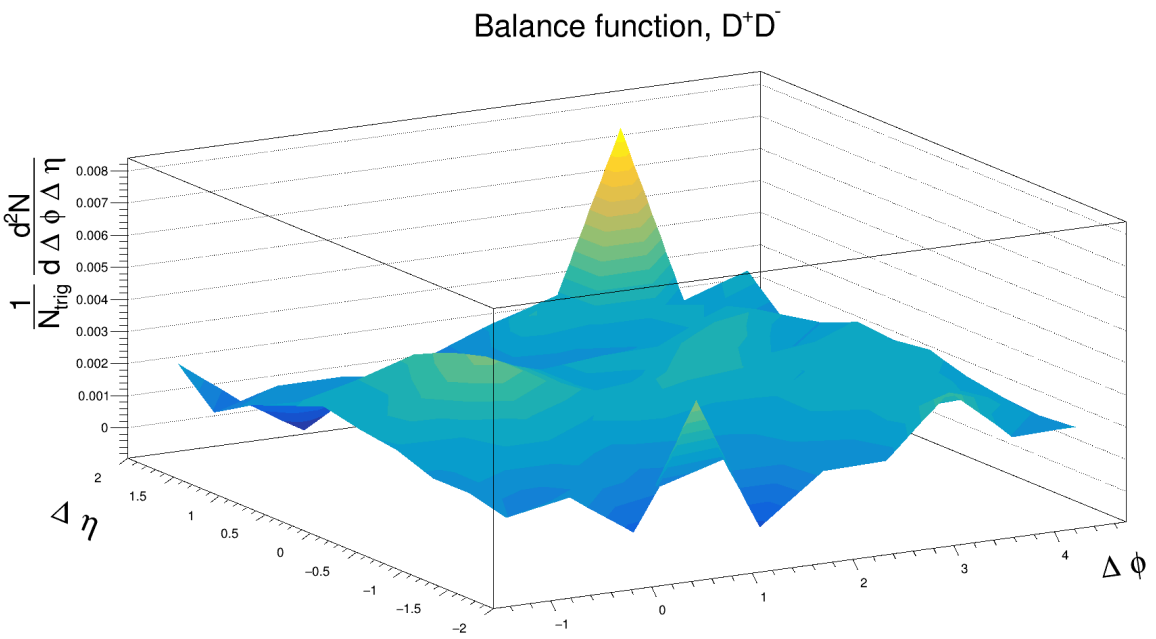

Figure A.4: D^+D^- balance function, 2D, sample 2

A.3 Forcing charm production, storing events with 4 charm quarks

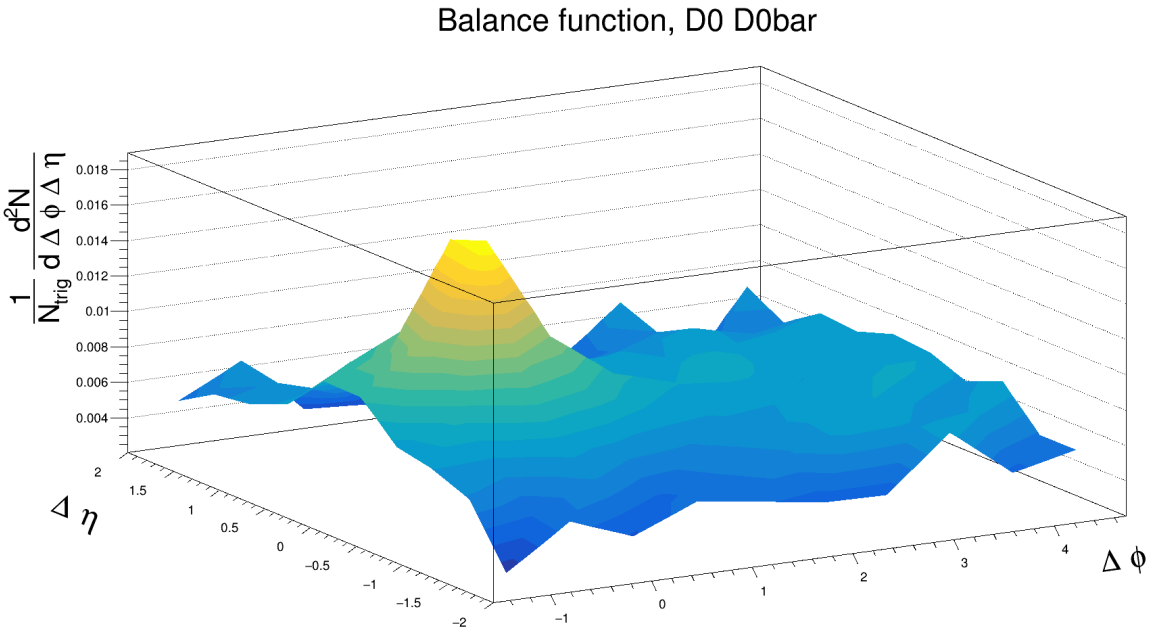

Figure A.5: $D^0\overline{D^0}$ balance function, 2D, sample 3

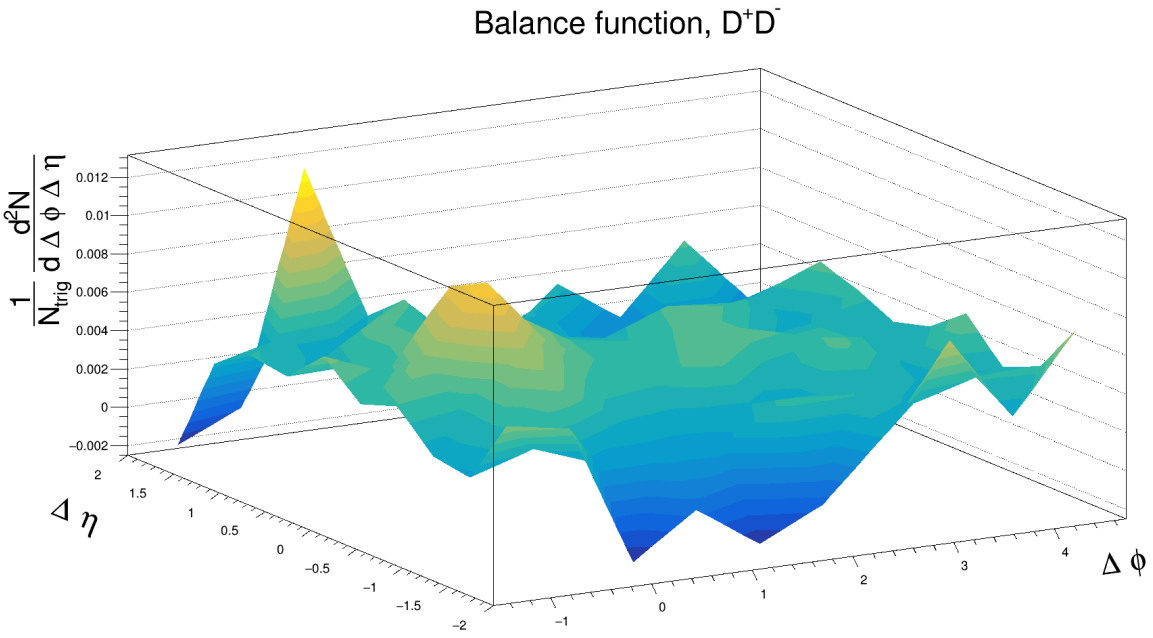

Figure A.6: D^+D^- balance function, 2D, sample 3

Appendix B

Plots with p_T cut

B.1 Minimum bias, storing events with 2 charm quarks

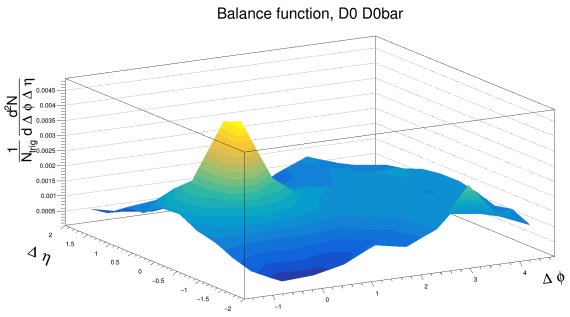

(a) $D^0\overline{D^0}$ balance function with p_T cut, 2D, sample 1

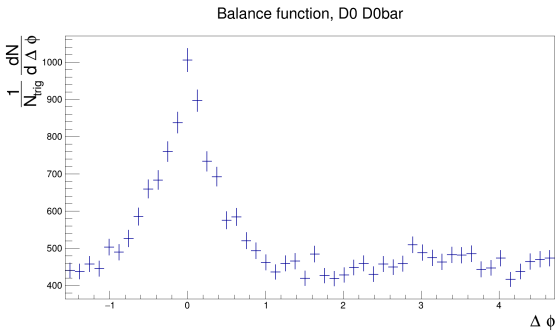

(b) $D^0\overline{D^0}$ balance function with p_T cut, 1D, sample 1

Figure B.1: $D^0\overline{D^0}$ balance function with p_T cut, sample 1

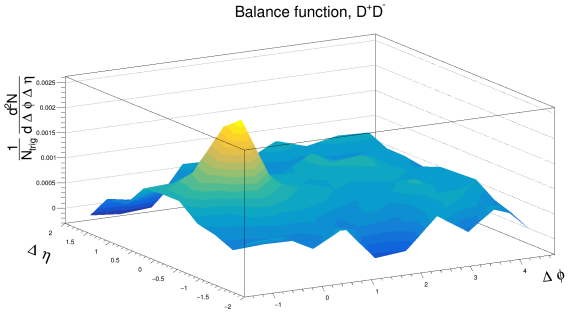

(a) D^+D^- balance function with p_T cut, 2D, sample 1

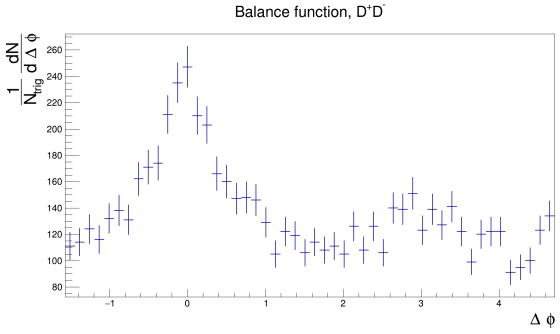

(b) D^+D^- balance function with p_T cut, 1D, sample 1

Figure B.2: D^+D^- balance function with p_T cut, sample 1

B.2 Forcing charm

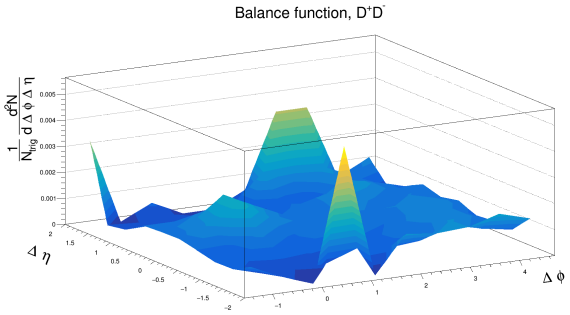

(a) D^+D^- balance function with p_T cut, 2D, sample 2

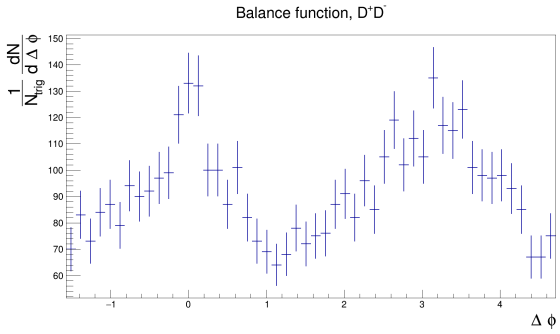

(b) D^+D^- balance function with p_T cut, 1D, sample 2

Figure B.3: D^+D^- balance function with p_T cut, sample 2

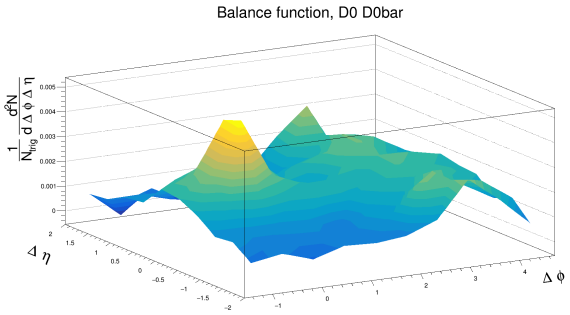

(a) $D^0\overline{D^0}$ balance function with p_T cut, 2D, sample 2

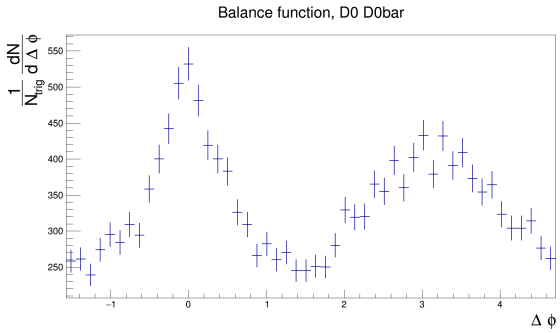

(b) $D^0\overline{D^0}$ balance function with p_T cut, 1D, sample 2

Figure B.4: $D^0\overline{D^0}$ balance function with p_T cut, sample 2

B.3 Forcing charm production, storing events with 4 charm quarks

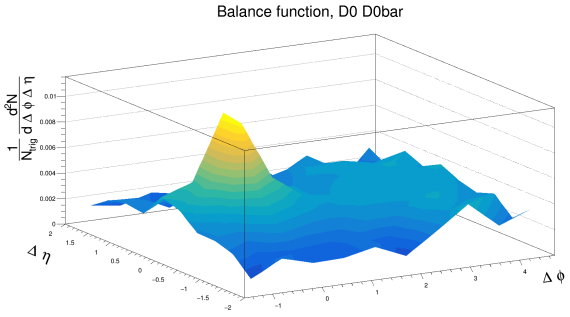

(a) $D^0\overline{D^0}$ balance function with p_T cut, 2D, sample 3

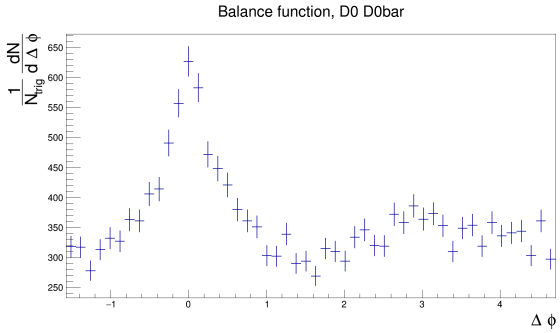

(b) $D^0\overline{D^0}$ balance function with p_T cut, 2D, sample 3

Figure B.5: $D^0\overline{D^0}$ balance function with p_T cut, sample 3

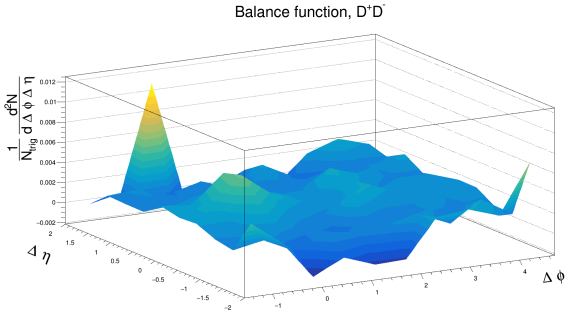

(a) D^+D^- balance function with p_T cut, 2D, sample 3

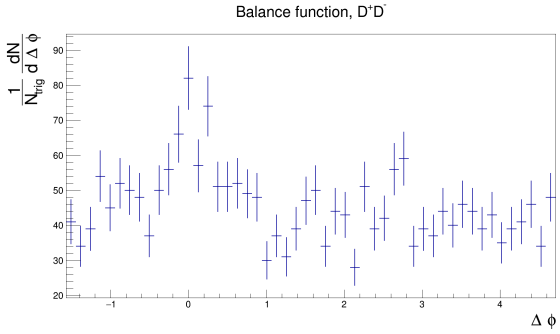

(b) D^+D^- balance function with p_T cut, 1D, sample 3

Figure B.6: D^+D^- balance function with p_T cut, sample 3